CEBAF Program Advisory Committee Six (PAC6) Proposal Cover Sheet

This proposal must be received by close of business on April 5, 1993 at:

CEBAF
User Liaison Office
12000 Jefferson Avenue
Newport News, VA 23606

Proposal Title

Measurement of the Magnetic Form Factor of the Neutron at Large Momentum Transfers

Contact Person

Name: Gerassimos G. Petratos

Institution: Stanford Linear Accelerator Center

Address: P.O. Box 4349, MS 20

Address: Stanford University

City, State ZIP/Country: Stanford, California 94309

Phone: (415) 926-4361 **FAX:** (415) 926-4999

E-Mail → BITnet: GGP@SLACVM **Internet:**

If this proposal is based on a previously submitted proposal or letter-of-intent, give the number, title and date:

CEBAF Use Only

Receipt Date: 4/5/93 Log Number Assigned: PR 93-024

By: gf

April 4, 1993

CEBAF Proposal - PAC6

MEASUREMENT OF THE MAGNETIC FORM FACTOR OF THE NEUTRON AT LARGE MOMENTUM TRANSFERS

THE HALL-A COLLABORATION*

Spokespersons: J. Gomez (*CEBAF*) and G. G. Petratos (*SLAC*)†

Abstract

We propose to extract the magnetic form factor of the neutron by exploring inclusive quasielastic electron-deuteron scattering to its practical limit of $Q^2 = 6.5$ $(\mathrm{GeV/c})^2$. The experiment will use the electron High Resolution Spectrometer and the deuterium/hydrogen cryotarget of Hall-A. The required beam energies range from 0.9 to 4.0 GeV. The spectrometer will be fixed at the backward scattering angle of 120° to eliminate any possible contributions to the quasielastic cross sections from the electric neutron form factor. We request 10 days of data taking calculated at 50% efficiency. The results will be of great importance in understanding the structure of the nucleons.

⋆ *Pending final approval at its May 93 Meeting.*

† *SLAC is not sponsoring this initiative as an Institution, given its policy of only supporting research activities at SLAC. The participation of G. G. Petratos is possible because of his fixed term research appointment at SLAC.*

1. INTRODUCTION

Over the past 40 years, the study of the underlying structure of the proton and neutron has been a major goal of nuclear and particle physics. Much of our understanding about the nucleon structure has come from elastic scattering of electrons interacting directly with the internal distribution of charge and magnetism in the nucleon. The electromagnetic probe has been a powerful microscope with a resolution, the momentum transfer in the interaction, limited only by the available accelerator energies.

Elastic electron-nucleon scattering is described, to lowest order in the fine coupling constant α, by the exchange of a single virtual photon. The differential cross section is given by the Rosenbluth formula:[1]

$$\frac{d\sigma}{d\Omega} = \frac{\alpha^2 E'}{4E^3 \sin^4(\frac{\theta}{2})} \left[(F_1^2 + \kappa^2 \tau F_2^2) \cos^2(\frac{\theta}{2}) + 2\tau (F_1 + \kappa F_2)^2 \sin^2(\frac{\theta}{2}) \right]$$

where E is the incident electron energy, E' is the scattered electron energy, θ is the scattering angle and κ is the anomalous magnetic moment of the nucleon. All the information about the nucleon structure is contained in the Dirac and Pauli form factors $F_1(Q^2)$ and $F_2(Q^2)$, respectively, with $Q^2 = 4EE' \sin^2(\theta/2)$ being the square of the four-momentum transferred to the nucleon. The kinematical factor τ is defined as $\tau = Q^2/4M^2$, where M is the nucleon mass. The Dirac form factor F_1 describes the distribution of charge and the normal part of the magnetic moment μ of the nucleon. The Pauli form factor describes the distribution of the anomalous part of the of the magnetic moment. The two form factors have been normalized at $Q^2 = 0$ to $F_1^p(0) = 1$, $F_2^p(0) = 1$ for the proton and $F_1^n(0) = 0$, $F_2^n(0) = 1$ for the neutron.

An alternative expression for the cross section is given in term of the Sachs[2] nucleon form factors $G_E(Q^2)$ and $G_M(Q^2)$:

$$\frac{d\sigma}{d\Omega} = \frac{\alpha^2 E'}{4E^3 \sin^4(\frac{\theta}{2})} \left[\frac{G_E^2 + \tau G_M^2}{1+\tau} \cos^2(\frac{\theta}{2}) + 2\tau G_M^2 \sin^2(\frac{\theta}{2}) \right]$$

The Sachs form factors $G_E(Q^2)$ and $G_M(Q^2)$ are referred to as the electric and magnetic form factors, respectively, because in the non-relativistic limit they are the Fourier transforms of the charge and magnetization distributions of the nucleons. They are normalized at $Q^2 = 0$ as follows: $G_E^p(0) = 1$, $G_M^p(0) = \mu_p = 2.79$ nm for the proton and $G_E^n(0) = 0$, $G_M^n(0) = \mu_n = -1.91$ nm for the neutron.

Early elastic electron-proton scattering[3] at low Q^2 uncovered the empirical dipole law and form factor scaling:

$$G_E^p(Q^2) \simeq \left(1 + \frac{Q^2}{Q_o^2}\right)^{-2} = G_D(Q^2)$$
$$G_M^p(Q^2) \simeq \left(1 + \frac{Q^2}{Q_o^2}\right)^{-2} \mu_p = G_D(Q^2)\mu_p$$

where $Q_o^2 = 0.71$ (GeV/c)^2. The form factor scaling indicated that the charge and magnetization distributions have the same spatial dependence. The dipole formula translated to an exponential spatial distribution with a rms radius $< r^2 >^{1/2} \simeq 0.81$ fm.

The low Q^2 measurements of the neutron magnetic form factor also showed that:

$$G_M^n(Q^2) \simeq \left(1 + \frac{Q^2}{Q_o^2}\right)^{-2} \mu_n = G_D(Q^2)\mu_n$$

indicating that the magnetic moment distribution of the neutron is similar to that of the proton. The neutron electric form factor measurements showed that $G_E^n(Q^2) \simeq 0$, indicating a zero net neutron charge distribution but also that the slope dG_E^n/dQ^2 is definitely > 0, indicating that the neutron charge distribution is not uniformly zero: the charge radius of the neutron is negative, *i.e.* there is a concentration of negative charge on the outside.

Since the first experiments that established the non-point like feature of the nucleons and their sizes, there has been an enormous continued experimental and theoretical work. The experimental work has focused into extending the form factor measurements at higher and higher momentum transfers and into improving their quality. The theoretical work has tried to explain or predict the behavior of the form factors within the contemporary nucleon models, ranging from the meson cloud picture to relativistic quark models.

The proton Sachs form factors have been separated[4] up to Q^2=9 (GeV/c)^2, as can be seen in Figure 1. The electric form factor is consistent with the dipole formula but the magnetic form factor shows a clear deviation from it. Data on the neutron form factors[5] exist only up to Q^2= 4 (GeV/c)^2 and are shown in Figure 2. The ratio G_E^n/G_D is consistent with zero; the neutron magnetic form factor is consistent with the dipole formula.

The objective of this proposal is to extend the measurements of the neutron elastic magnetic form factor, by exploring backward inclusive quasielastic electron-deuteron scattering to its practical limit of about Q^2= 6.5 (GeV/c)^2. The choice of a backward scattering angle will eliminate any possible contribution from the electric neutron form factor. The results will be limited by theoretical uncertainties in modeling the deuteron wave function and the inelastic scattering background to the quasielastic cross sections, rather than statistical or experimental uncertainties. The new data will impose severe constraints in the theoretical calculations of the nucleon form factors.

2. THEORY

The first attempt to describe theoretically the nucleon form factors was within the framework of Vector Meson Dominance (VMD). In the VMD picture, the virtual photon couples to the nucleon through vector mesons (see Figure 3) and the nucleon form factors are expressed in terms of photon-meson coupling strengths $C_{\gamma V}$ and meson-nucleon vertex form factors F_{VN}:

$$F(Q^2) = \sum_j \frac{m_j^2 C_{\gamma V_j}}{m_j^2 + Q^2} F_{V_iN}(Q^2)$$

where the sum is over all possible vector mesons of mass m_j. VMD parametrizations,[29][6,7] though with flexibility in the choice of parameters, have given fair descriptions of the low Q^2 data, as can be seen in Figures 1 and 2.

A common problem with the VMD models is that they do not incorporate a proper description of the nucleon form factors at large Q^2. Since the advent of the quark-parton model and Quantum Chromodynamics (QCD), it is believed that at large Q^2 the nucleons must behave as bound systems of point-like quarks governed by the properties of the strong force. Beginning with the pioneering work of Brodsky and Farrar[8] as well as Matveev *et. al.*,[9] alternative theoretical calculations for the nucleon form factors based on quark dimensional scaling laws and perturbative QCD have emerged.

Dimensional scaling[8] predicts that, at large Q^2, only the valence quark states are important in exclusive processes such as elastic electron-nucleon scattering. The underlying dynamical mechanism is the hard rescattering of the quarks that constitute the nucleons, shown in Figure 3. In this case, a rough idea of the Q^2 dependence can be gained by simply counting the number of gluon propagators. The Dirac F_1 form factor, for example, should scale asymptotically as $(Q^2)^{-(n-1)}$, where $n = 3$ is the number of valence quarks. Large Q^2 SLAC data[10] are consistent with this prediction as can be seen in Figure 4.

The simple quark counting rules were later justified within the framework of perturbative QCD. It was demonstrated[11] that, at large Q^2, QCD effects produce only a logarithmic departure from the dimensional scaling power-laws. Within the hard scattering scheme, the nucleon form factors are written as a convolution of distribution amplitudes, representing the scattering of constituents in a collinear approximation. Naive symmetric distribution amplitudes where the three valence quarks share equally the nucleon's momentum failed dramatically to account for the sign and normalization of the proton magnetic form factor. Agreement with the data can be achieved only with a distribution amplitude in which the momentum balance of the valence quarks in the proton is quite asymmetric.[12]

The apparent success of perturbative QCD for asymmetric distribution amplitudes is achieved at the expense of strong contributions from 'soft' regions where one of the constituents carry a small fraction of the nucleon's momentum. This is, as has been pointed out by Isgur and Llewellyn-Smith,[33] a very problematic situation for a calculation relying on perturbation theory. Although the hard scattering picture is likely to be the true asymptotic description for the nucleon form factors, it needs modifications at moderate momentum transfers.

Nesterenko and Radyushkin[34] have attempted to calculate the contribution to the nucleon form factors from soft non-perturbative processes. They fixed the soft nucleon wave functions by employing QCD sum rules[14] based on quark-hadron duality. They decomposed the scattering process in the series of diagrams of Figure 5. Their calculation showed that the contribution from just diagram a) is enough to describe the moderate Q^2 e-p data. At large Q^2, diagrams a) and b) are suppressed due to momentum imbalance at the quarks and diagram c) becomes dominant. They estimated that the scale of the transition could be of the order $Q^2 = 100$ (GeV/c)^2.

To describe the moderate momentum transfer region, Kroll, Schürmann and Schweiger[32] proposed a generalization to the hard scattering scheme by modeling nucleons as made of quarks and diquarks. The diquarks are treated as quasi-elementary constituents which partly survive medium hard collisions. Their composite nature is taken into account by diquark form factors. The diquarks are viewed as an effective description of correlations in the nucleon wave function and constitute a model for non-perturbative effects. The model is designed such that, at large momentum transfers, when the diquarks dissolve into quarks, perturbative QCD emerges.

Recently, there have been two exploratory calculations[33][15] to describe the nucleon form factors in the intermediate Q^2 range in the light of relativistic constituent-quark models. Both calculations use a particular nucleon wave function model with two parameters: the effective quark mass m and a confinement scale a. For example, the model by Chung and Coester assumes a simple exponential wave function of the form $\phi(M_o) = N \exp\,(-M_o^2/2a^2)$ where $M_o^2 = \sum_i \sqrt{m_i^2 + \vec{q}_i^{\,2}}$ with $\vec{q}_i$ being the quark relative momenta. The model of Schlumpf assumes also a symmetric wave function of a particular form. The confinement scale a is of the order of 0.6 GeV and the quark mass that reproduces (partially) the data is ~0.25 GeV, smaller than the conventional non-relativistic choice of 1/3 of the nucleon mass.

There have been also hybrid phenomenological approaches to describe the moderate Q^2 regime[31][16] by synthesizing in a direct way the meson picture of VMD and quark picture of perturbative QCD using parametrizations of the form factors which properly combine these two pictures. For example, Gari and Krümpelmann[31] modify their VMD formalism for F_1, which includes only ω and ρ mesons, by a multiplicative factor containing two parameters (determined from fits to data) Λ_1 and Λ_2:

$$F_1^{QCD} = \frac{\Lambda_1^2}{\Lambda_1^2 + \widehat{Q}^2} \frac{\Lambda_2^2}{\Lambda_2^2 + \widehat{Q}^2}$$

Λ_1 is the scale of the nucleon wave function ($\sim$ 0.8 GeV) and Λ_2 is the scale of the transition from meson dynamics to quark dynamics ($\sim$ 5 (GeV/c)^2). The parameter $\widehat{Q}^2$ contains the logarithmic dependence of the strong coupling constant $\alpha_s(Q^2)$.

3. THE EXPERIMENT

We propose to measure electron-deuteron quasielastic scattering at a fixed scattering angle of 120° up to the maximum laboratory energy of 4 GeV. The selection of the angle is such that any possible contribution to the cross section from the neutron electric form factor vanishes. At 120°, the upper limit values of G_E^n from the cross sections measured in SLAC experiment E-133[17] produce a negligible contribution to the cross sections. At every energy setting, we will also measure elastic as well as inelastic electron-proton scattering in order to subtract the proton quasielastic and the deuterium inelastic contributions to the cross sections.

The neutron magnetic form factor will be extracted from the radiatively corrected measured inclusive spectra, after subtracting the inelastic contributions. These contributions will be calculated using a Fermi-smearing model to convolute the measured proton resonance region data with the deuteron wave function. The convoluted spectra will be fitted to the deuterium data in the same region.

We will use the electron High Resolution Spectrometer (HRS) of Hall-A with its standard detection package being built. The package consists of a drift chamber set for track reconstruction, a pair of hodoscopes for triggering and fast timing, and a gas threshold Čerenkov counter and a lead glass shower counter for electron identification. The above two counters are expected to provide a pion rejection factor of $> 10^4$ in the energy range of 0.5 GeV. Extrapolation of the measured π/e ratios of SLAC experiment NE-11[5] to the conditions of this experiment leads to an expected ratio of 2-3 $\times 10^2$ in the worst case, resulting in a negligible pion contamination to the electron spectra. Contributions to the cross sections by electrons from charge symmetric processes, such as π_o decays, will be measured by reversing the spectrometer polarity and measuring the positron yields.

To minimize the time required to perform the experiment, we plan to use the large solid angle tune[18] of HRS where the two front quadrupoles are moved towards the target by $\simeq$ 1 m. This tune will provide a solid angle of $\sim$ 15 msr. The momentum and angular resolutions of this tune suffice for the needs of this experiment. Typically, 3 to 4 overlapping spectrometer momentum settings will be required to cover the quasielastic peaks.

To maximize the counting rate, we will use the high-power cryotarget of Hall-A now being built. The target cell will have a length of 15 cm. Assuming a realistic beam current of 100 μA (half the accelerator design value), the power deposited in the target will be $\sim$ 500 W for deuterium and $\sim$ 430 W for hydrogen. The current refrigeration plans for the cryotarget allow for a heat dissipation of $\sim$ 500 W, sufficient for the needs of this experiment. The contribution to the counting rate from the target cell endcaps will be eliminated by using two tungsten collimators.

They will mask the spectrometer from the endcaps and at the same time will define the effective target length seen by the spectrometer.

4. EXTRACTION OF THE NEUTRON FORM FACTOR

The elastic electron-neutron cross sections and the magnetic form factor of the neutron will be extracted from the measured electron-deuteron inclusive cross sections around the quasielastic peak through a fitting procedure based on the following assumption: The measured electron-deuteron cross section σ_{ed} is the sum of the cross sections from three processes: 1) quasielastic electron-proton scattering, 2) quasielastic electron-neutron scattering and 3) inelastic electron-deuteron scattering.

The smeared proton cross sections $(\sigma_{ep})_s^q$ from the first process can be generated by the measured e-p elastic cross sections taking into account the smearing caused by the nucleon binding in the deuteron. The Fermi motion of the struck nucleons is incorporated from the deuteron wave functions of phenomenological realistic nucleon-nucleon potentials using the PWIA McGee-Durand formalism:[19]

$$(\sigma_{ep})_s^q = \sigma_{ep}\frac{M^2}{2q}\frac{E}{E'}\int_{k_{min}}^{k_{max}} \frac{\left[u^2(k)+v^2(k)\right]k}{\sqrt{k^2+M^2}}dk \tag{4.1}$$

where σ_{ep} is the elastic e-p cross section and q is the magnitude of the momentum transfer $\vec{q} = \vec{E} - \vec{E}'$. The functions $u(k)$ and $v(k)$ are the s-wave and d-wave components of the deuteron wave function, where k is the momentum of the struck nucleon along the direction of $\vec{q}$. The smeared neutron cross sections $(\sigma_{en})_s^q$ from the second process are assumed to be proportional to the smeared proton cross sections: $(\sigma_{en})_s^q = a_1(\sigma_{ep})_s^q$.

The contribution from the third process can be calculated from measured inelastic e-p cross sections. This process can be considered as the sum of Fermi-smeared inelastic e-p and Fermi-smeared inelastic e-n scattering. The inelastic e-n

cross sections are assumed to be proportional to the inelastic e-p cross. The inelastic e-p cross sections will be measured in the experiment. There are currently two Fermi-smearing algorithms to calculate the inelastic $(\sigma_{ed})^i_s$ contribution.

The first method utilizes the incoherent impulse approximation formalism of Atwood-West[20] as given by Bodek.[21] In this approximation, only one nucleon is directly engaged in the scattering process (the interaction nucleon), while the other nucleon (the spectator nucleon) is unaffected. The spectator nucleon is on the mass shell before and after the interaction, while the interaction nucleon is initially off the mass shell and is brought back on the mass shell by the absorption of the virtual photon. The smeared inelastic structure functions $(W_1)_s$ and $(W_2)_s$ of the deuteron are then calculated from a model of the nucleon inelastic structure functions $W_1^{p,n}$ and $W_2^{p,n}$ and the deuteron wave function. For example:

$$(W_1)_s = \sum\nolimits_{p,n} \int \left(u^2(k) + v^2(k)\right) \left[W_1^{p,n} + W_2^{p,n} \frac{k_\perp^2}{2M^2}\right] dk$$

A similar expression holds for $(W_2)_s$. The authors also prescribe modifications to $W_1^{p,n}$ and $W_2^{p,n}$ to include possible off-mass shell effects. This method has been also used in extracting the ratio σ_n/σ_p from the SLAC deep inelastic experiments.[21]

The second method, developed by Sargsian, Frankfurt and Strikman,[22] is based on an impulse approximation approach using light-cone quantum mechanics and its associated light-cone variables. This method gives results similar to the previous one. For example, $(W_1)_s$ is calculated to be:

$$(W_1)_s = \sum_{p,n} \int \left(u^2(k) + v^2(k)\right) \frac{2M}{aM_d} \left[W_1^{p,n} + W_2^{p,n} \frac{k_\perp^2}{2M^2}\right] dk$$

where M_d is the deuteron mass and $(1 - a/2)$ is the fraction of the deuteron momentum carried by the spectator nucleon. The authors give also prescriptions to account for a possible EMC effect in the deuteron and for a correction to the normalization of the deuteron wave function based on baryon charge conservation.[23]

Finally, at each incident beam energy the measured cross section will be expressed as:

$$\sigma_{ed} = (1 + a_1)(\sigma_{ep})^q_s + a_2(\sigma_{ed})^i_s \tag{4.2}$$

and a least-squares fit will determine the value of the ratio $a_1 = (\sigma_{en}/\sigma_{ep})^q_s$ using the data around the top of the quasielastic peak. The neutron magnetic form factor G^n_M will be then calculated from the ratio a_1 using values for the proton magnetic form factor G^p_M which will be extracted from this experiment, and the G^p_E values from SLAC experiment NE-11[4] and/or CEBAF experiment 89-14.[24]

5. RUN PLAN - ERRORS

The proposed kinematics for the G^n_M measurements in the Q^2 range from 1.0 to 6.5 (GeV/c)^2 is given in Table 1. The required beam energies range from 0.9 to 4.0 GeV. The HRS momentum settings will vary from 0.30 to 0.63 GeV/c. To calculate counting rates, we have used the proton form factor values of SLAC experiment NE-11[4] and assumed that the neutron magnetic form factor follows the dipole formula and that the neutron electric form factor is zero. The counting rates are integrated over the quasielastic peaks and assume 100 μA beam current, a 15 cm long liquid deuterium target, a solid angle of 15 msr for HRS and a radiative correction factor of 0.7.

A 1% statistical precision in the measurement of G^n_M will require collection of about 50,000 quasielastic events at each energy setting. Based on the above assumptions, the required time for the inclusive *e-d* measurements will be 56 hours. The measurements of the proton magnetic form factor will require 19 hours assuming a 15 cm liquid hydrogen target. The measurements of inelastic electron-proton scattering will require 22 hours. An additional 20 hours will be required for positron measurements. Assuming a 50% data collection efficiency, the estimated required time to perform the measurements will be 10 days.

We estimate that the total systematic error in the measurement of G_M^p will be about 2% by adding in quadrature the uncertainties in target length ($\sim$ 1%), incident beam current ($\sim$ 1%), spectrometer solid angle ($\sim$ 1%) and radiative corrections ($\sim$ 1.5%). The statistical error will be in all cases $\leq$ 1%. The uncertainties in absolute incident and scattered electron energies, in scattering angle, as well as in the assumed value of G_E^p will introduce, at the backward scattering angle of 120°, a negligible error in the extraction of G_M^p. The contribution of the electric form factor G_E^p to the measured elastic e-p cross section will be about 1%.

The total systematic error in the inclusive electron-deuteron cross sections is estimated to be about 3% by adding in quadrature the dominant uncertainties in target length ($\sim$ 1%), incident beam current ($\sim$ 1%), spectrometer solid angle ($\sim$ 1%) and radiative corrections ($\sim$ 2%). The overall experimental uncertainty in the extraction of G_M^n will be about 5% including the propagation of the total error in the measurement of G_M^p. The G_M^n statistical uncertainty for all kinematics will be about 1%. The quality of the projected possible CEBAF data under the above assumptions is shown in Fig. 6.

The sensitivity to the deuteron non-relativistic PWIA wave function has been modeled using the standard McGee-Durand formalism with four realistic nucleon-nucleon potentials: Paris,[25] Bonn,[26] Reid Soft Core[27] and Lomon-Feshbach with 5.2% d-state.[28] It was found to be of the order of 2-3% and independent of Q^2. The sensitivity to recent relativistic Impulse Approximation calculations has been examined in the analysis of SLAC experiment NE-11. A model by Chung and Coester[5] changed the G_M^n results by -1.2% at Q^2=1.75 (GeV/c)^2 and by +1.4% at Q^2=4 (GeV/c)^2 (relative to the McGee-Durand model). A model by Gross and Van Orden[5] caused a bigger change: 5.7% on the average (independent of Q^2), but gave significantly worse χ^2 fits.

The sensitivity to the inelastic modeling has been studied by Sargsian, Frankfurt and Strikman,[22] in extracting the ratio of the elastic cross sections σ_n/σ_p and the value of G_M^n (assuming $G_E^n = 0$) from the forward (8°) data of SLAC experiment E-133. They estimated that the uncertainty in G_M^n is about 6-7% at Q^2=6.5 (GeV/c)^2 and concluded that inclusive $(e,e')d$ scattering provides a reliable method for extracting G_M^n for $Q^2 \lesssim 6$ (GeV/c)^2. Similar conclusions were drawn in the analysis of SLAC experiment NE-11[5], for its kinematic range, using either the same or the Atwood-West formalism. The contribution to the measured cross sections at the top of the quasielastic peak from inelastic processes will range from 1% at $Q^2 = 1$ (GeV/c)^2 to an estimated 25% at Q^2=6.5 (GeV/c)^2.

All modeling studies indicate that even at the highest Q^2=6.5 (GeV/c)^2 of the proposed experiment, the theoretical error in the extraction of the neutron form factor from quasielastic e-d scattering will be less than 10%. For comparison, it should be noted that most of the existing low Q^2 data on G_M^n have comparable errors. The proposed data will be of precision sufficient to put severe constraints in the theoretical calculations of the neutron structure.

6. SUMMARY - REQUEST

We propose to extract the magnetic form factor of the neutron from inclusive quasielastic electron-deuteron scattering up to the maximum practical momentum transfer of 6.5 (GeV/c)^2, limited by theoretical uncertainties. The experiment will use the electron High Resolution Spectrometer and the deuterium/hydrogen cryotarget of Hall-A. The required beam energies range from 0.9 to 4.0 GeV. The spectrometer will be fixed at the backward scattering angle of 120° to eliminate any possible contributions to the quasielastic cross sections from the electric neutron form factor. We request 10 days of data taking based on 50% efficiency plus 3 days of checkout time. The results will have a significant impact in testing our understanding of the structure of the neutron.

TABLE CAPTIONS

1: Quasielastic electron-deuteron and elastic electron-proton kinematics in the momentum transfer Q^2 range 1.0 to 6.5 $(\text{GeV/c})^2$, and counting rates. The electron scattering angle is fixed at 120°. E is the incident beam energy and E' is the scattered electron momentum. The cross sections assume the proton form factor values of SLAC experiment NE-11[4] and that the neutron magnetic form factor follows the dipole formula meanwhile the electric form factor is zero. The counting rates are integrated over the quasielastic peak and assume a 15 cm long liquid deuterium/hydrogen target, a beam current of 100 μA, 15 msr solid angle for HRS and a radiative correction factor of 0.7.

TABLE 1

G_M^n RUN PLAN SCENARIO

$\theta = 120°$

Target = 15 cm Liquid Deuterium/Hydrogen

Current = 100 μA

$\Delta\Omega$ = 15 msr

Q^2 $(\mathrm{GeV/c})^2$	E (GeV)	E' (GeV)	Time (hour)	Quasielastic Counts	Time (hour)	e-p Elastic Counts
1.00	0.902	0.369	2	50000	1	10000
1.50	1.212	0.413	2	50000	1	10000
2.00	1.508	0.442	2	50000	1	10000
2.50	1.796	0.464	2	50000	1	10000
3.00	2.080	0.481	2	50000	1	10000
3.50	2.360	0.494	2	50000	1	10000
4.00	2.637	0.506	3	50000	1	10000
4.50	2.913	0.515	3	50000	1	10000
5.00	3.187	0.523	5	50000	1	10000
5.50	3.461	0.530	7	50000	2	10000
6.00	3.733	0.536	10	50000	3	10000
6.50	4.005	0.541	15	50000	4	10000
TOTAL			56		19	
TOTAL	50%	Efficiency	112		38	

FIGURE CAPTIONS

1) Data on the proton electric and magnetic form factors. Also shown are theoretical calculations: the VMD model by Iachello, Jackson and Lande[29] (IJL, dotted curves), the fit of Höhler *et. al.*[30] (H, long-dash curves), the parametrization by Gari and Krümpelmann[31] (GK, solid curves), the diquark model of Kroll, Schürmann and Schweiger[32] (KSS, short-dash curves), the relativistic constituent-quark model of Chung and Coester[33] (CC, dash-double dotted curves) and the Nesterenko and Radyushkin QCD Sum Rule predictions[34] (R, dash-dotted curves).

2) Data on the neutron electric and magnetic form factors. Also shown are theoretical calculations: the VMD model by Iachello, Jackson and Lande[29](IJL, dotted curves), the fit of Höhler *et. al.*[30](H, long-dash curves), the parametrization by Gari and Krümpelmann[31](GK, solid curves), the diquark model of Kroll, Schürmann and Schweiger[32](KSS, short-dash curves), the relativistic constituent-quark model of Chung and Coester[33](CC, dash-double dotted curves) and the Nesterenko and Radyushkin QCD Sum Rule predictions[34](R, dash-dotted curves).

3) Elastic electron-nucleon scattering a) in the Vector Meson Dominance (VMD) scheme, where the virtual photon that mediates the interaction couples to the nucleon through vector mesons; b) in the hard scattering scheme of Quantum Chromodynamics.

4) The proton F_1 form factor at large Q^2 extracted from SLAC cross section measurements[10] at forward scattering angles assuming form factor scaling. Dimensional scaling[8] predicts that at large momentum transfers the product $Q^4 F_1^p$ should approach a constant value.

5) The quark-gluon factorization scheme describing elastic electron-nucleon scattering in the framework of Quantum Chromodynamics.

6) Projected possible data for the measurement of G_M^n at CEBAF using the

electron High Resolution Spectrometer (HRS) of Hall-A. The run plan assumes the 15 msr large solid angle tune of HRS, a 15 cm long deuterium cryotarget and 100 μA electron beam current. The required beam time is 10 days including proton calibrations, assuming 50% data taking efficiency.

REFERENCES

1. M. N. Rosenbluth, Phys. Rev. **79**, 615 (1950).
2. F. J. Ernst, R. G. Sachs and K. C. Wali, Phys. Rev. **119**, 1105 (1960).
3. R. Hofstadter, Ann. Rev. Nucl. Sci. **7**, 231 (1957).
4. P. E. Bosted *et. al.*, Phys. Rev. Lett. **68**, 3841 (1992), and references therein.
5. A. F. Lung *et. al.*, Phys. Rev. Lett. **70**, 718 (1993), and references therein.
6. J. G. Körner and M. Kuroda, Phys. Rev **D16**, 2165 (1977).
7. S. Blatnik and N. Zovko, Acta Phys. Austriaca **39**, 62 (1974).
8. S. J. Brodsky and G. Farrar, Phys. Rev. Lett. **31**, 1153 (1973); Phys. Rev. **D11**, 1309 (1975).
9. V. A. Matveev, R. M. Muradyan and A. N. Tavkhelidze, Lett. Nuovo Cimento **7**, 719 (1973).
10. A. F. Sill *et. al.*, SLAC-PUB-4395 (1992).
11. G. P. Lepage and S. J. Brodsky, Phys. Rev. **D22**, 2157 (1980).
12. V. L. Chernyak and I. R. Zhitnitsky, Nucl. Phys **B246**, 52 (1984).
13. N. Isgur and C. Llewellyn-Smith, Phys. Rev. Lett. **52**, 1080 (1984); Phys. Lett. **B217**, 535 (1989).
14. M. A. Shifman, A. I. Vainshtein and V. I. Zakharov, Nucl. Phys. **B147**, 385 (1979).
15. F. Schlumpf, SLAC-PUB-5968 (1992); SLAC-PUB-6050 (1993).
16. S. Furuichi and K. Watanabe, Prog. Theor. Physics **82**, 581 (1989); **83**, 565 (1990).
17. S. E. Rock *et. al.*, Phys. Rev. **D46**, 24 (1992).
18. *Conceptual Design Report, CEBAF Basic Experimental Equipment*, p. A4-13 (1990).

19. I. McGee, Phys. Rev. **161**, 1640 (1967); L. Durand III, Phys. Rev. Lett. **6**, 631 (1961); A. F. Lung, SLAC-NPAS-TN-91-2 (1991).

20. W. B. Atwood and G. B. West, Phys. Rev. **7**, 773 (1973).

21. A. Bodek *et. al.*, Phys Rev. **20**, 1471 (1979).

22. M. M. Sargsian, L. L. Frankfurt and M. I. Strikman, Z. Phys. **A335**, 431 (1990).

23. L. L. Frankfurt and M. I. Strikman, Phys. Lett. **64B**, 433 (1976).

24. CEBAF Proposal 89-14, The Hall-A Collaboration, spokespersons: C. F. Perdrisat and V. Punjabi (1989).

25. M. Lacombe *et. al.*, Phys. Lett. **101B**, 139 (1981).

26. R. Machleidt, K. Holinde and C. Elster, Phys. Rep. **149**, 1 (1987).

27. R. V. Reid, Jr., Ann. Phys. (N.Y.) **50**, 411 (1968).

28. E. Lomon and H. Feshbach, Ann. Phys. (N.Y.) **48**, 94 (1968).

29. F. Iachello, A. Jackson and A. Lande, Phys. Lett. **43B**, 191 (1973).

30. G. Höhler *et. al.*, Nucl.Phys. **B114**, 505 (1976).

31. M. Gari and W. Krümpelmann, Z. Phys. **A322**, 689 (1985); Phys. Lett. **B173**, 10 (1986).

32. P. Kroll, M. Schürmann and W. Schweiger, Z. Phys. **A338**, 339 (1991).

33. P. L. Chung and F. Coester, Phys. Rev. **D44**, 229 (1991).

34. V. A. Nesterenko and A. V. Radyushkin, Phys. Lett **128B**, 439 (1983); Sov. J. Nucl. Phys. **39**, 811 (1984).

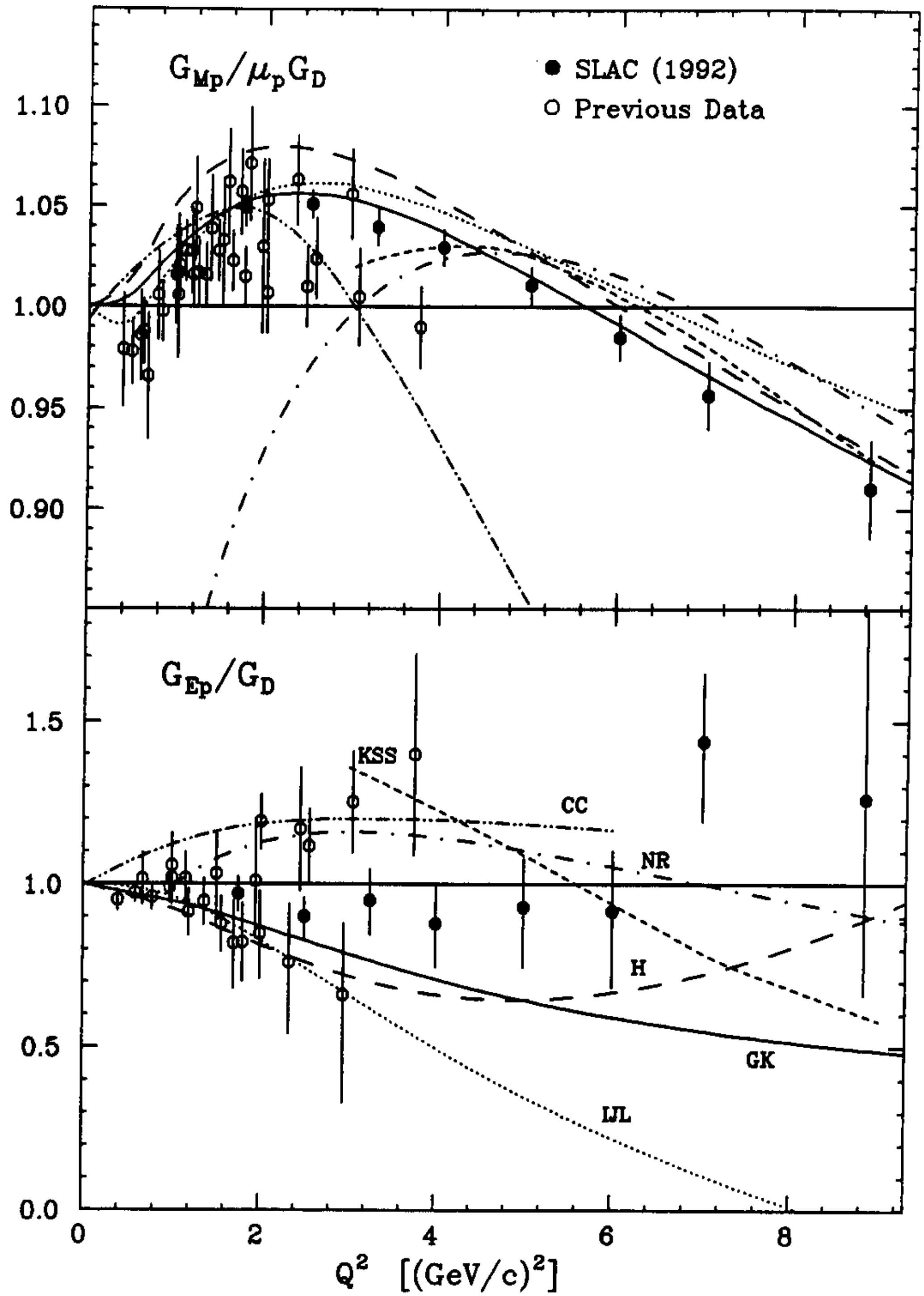

$G_{Mp}/\mu_p G_D$
SLAC (1992)
Previous Data
1.10
1.05
1.00
0.95
0.90
G_{Ep}/G_D
1.5
1.0
0.5
0.0
KSS
CC
NR
H
GK
IJL
0
2
4
6
8
Q^2 $[(GeV/c)^2]$

Figure 1

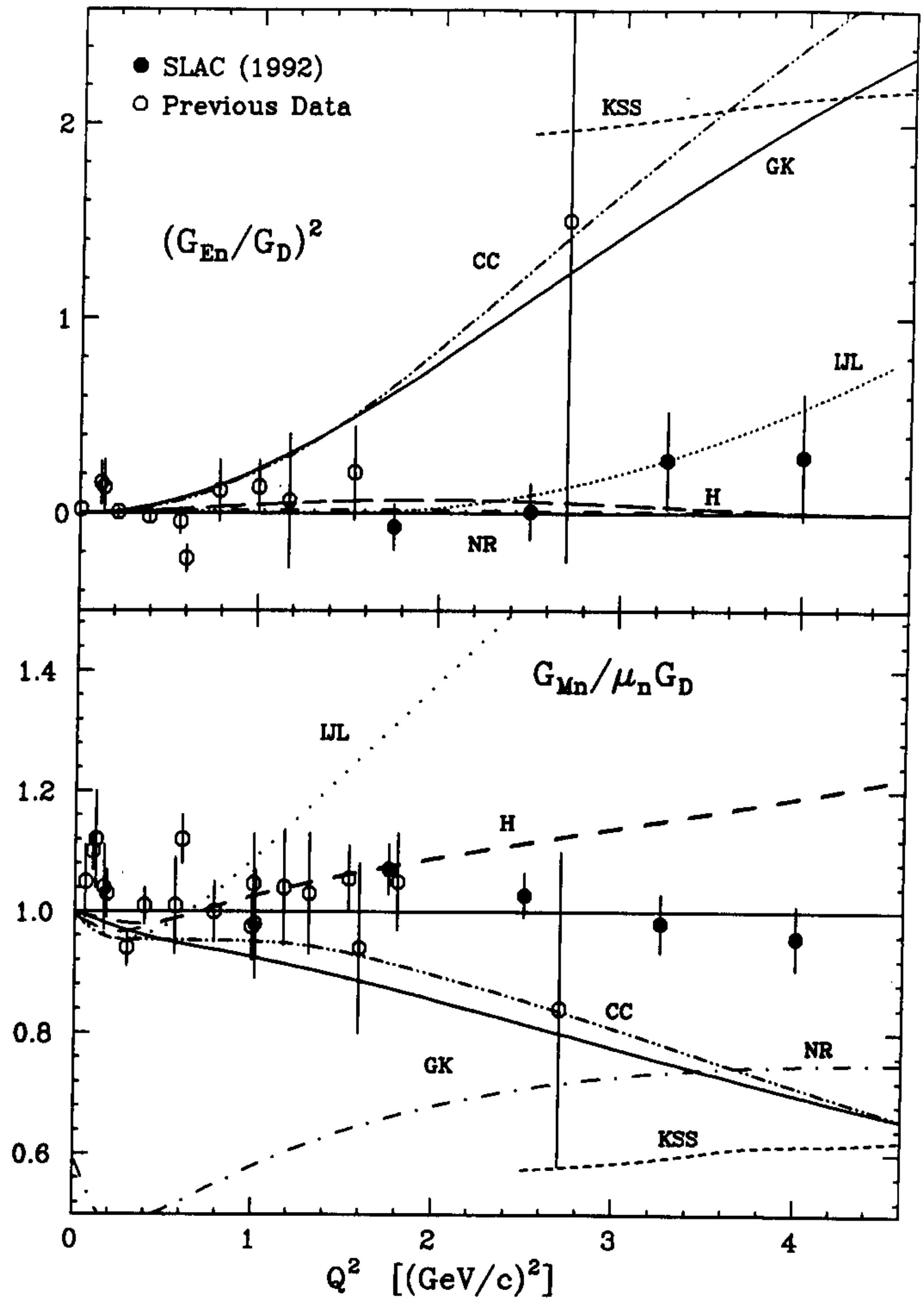

SLAC (1992)
Previous Data
$(G_{En}/G_D)^2$
KSS
GK
CC
IJL
H
NR
2
1
0
$G_{Mn}/\mu_n G_D$
IJL
H
CC
NR
GK
KSS
1.4
1.2
1.0
0.8
0.6
0
1
2
3
4
Q^2 $[(GeV/c)^2]$

Figure 2

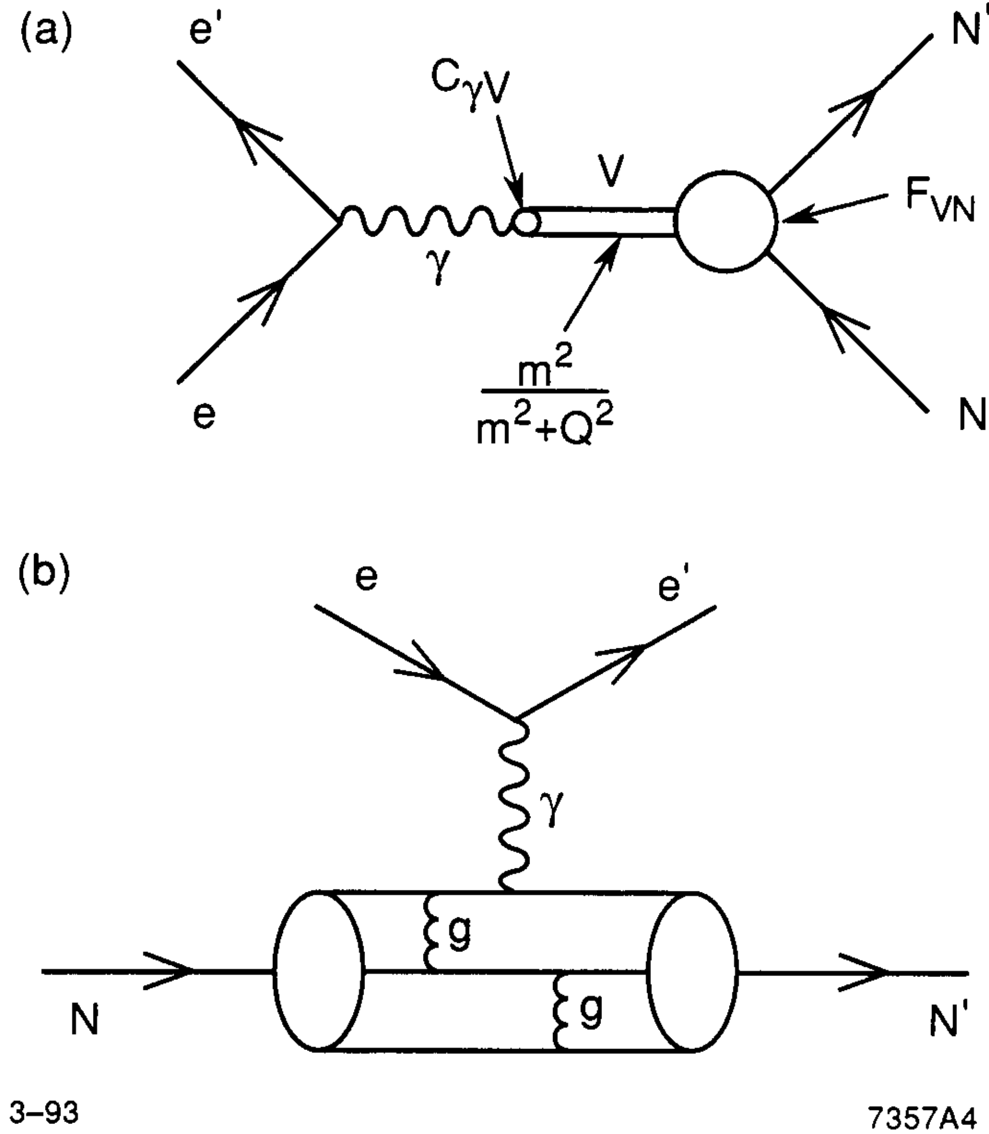

(a)
e'
$C_{\gamma V}$
V
N'
F_{VN}
γ
$\frac{m^2}{m^2+Q^2}$
e
N
(b)
e
e'
γ
g
g
N
N'
3–93
7357A4

Figure 3

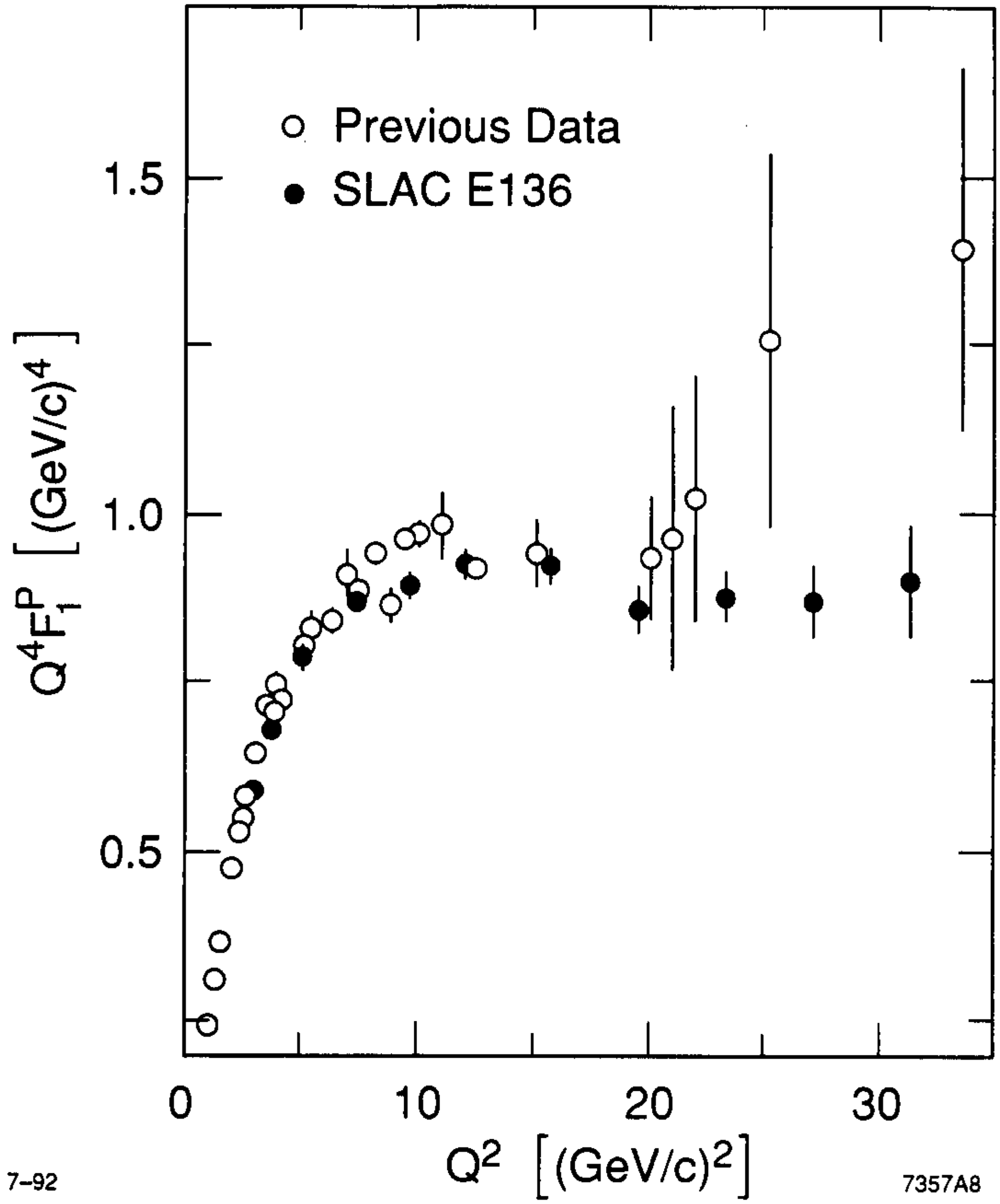

Previous Data
SLAC E136
1.5
1.0
0.5
0
10
20
30
$Q^4F_1^P$ [$(GeV/c)^4$]
Q^2 [$(GeV/c)^2$]
7-92
7357A8

Figure 4

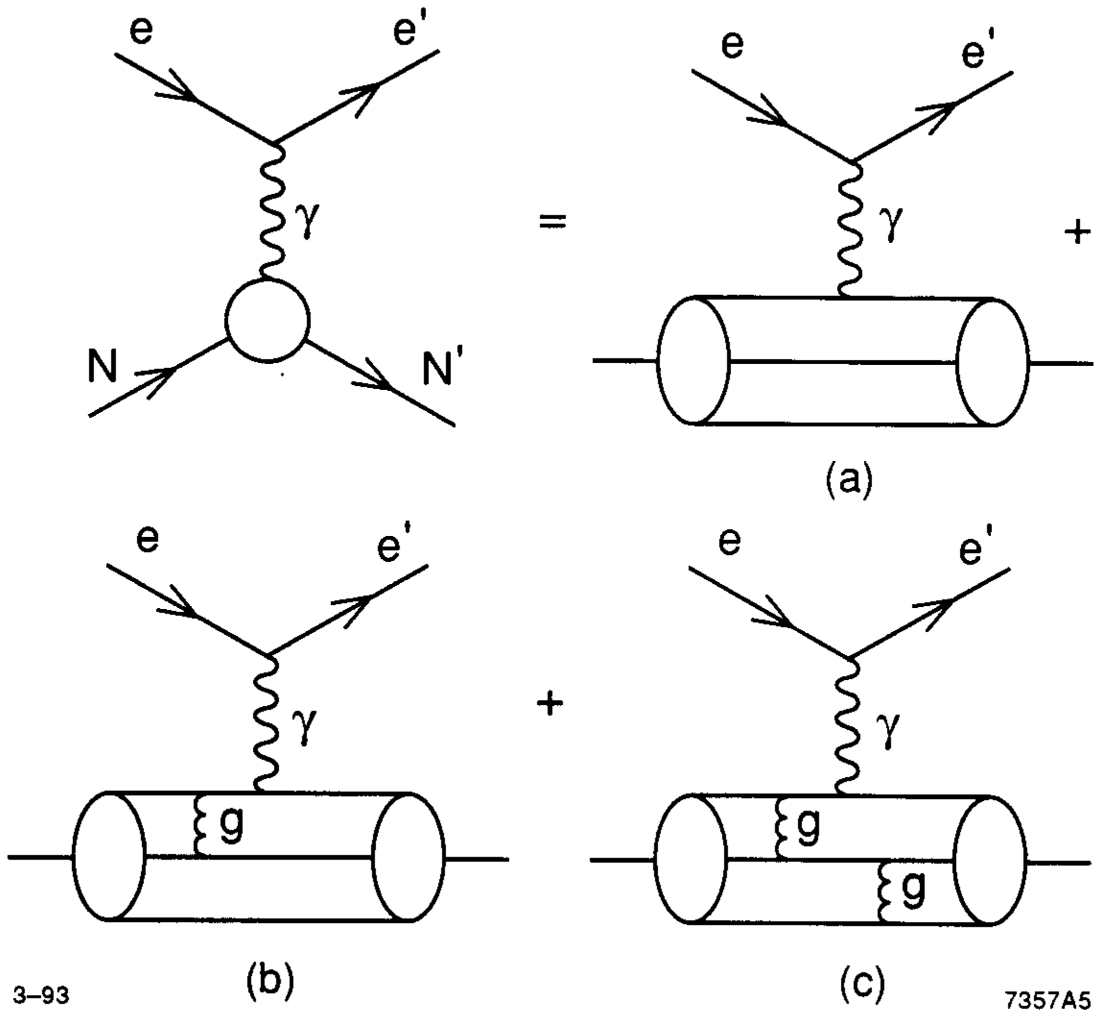

Figure 5

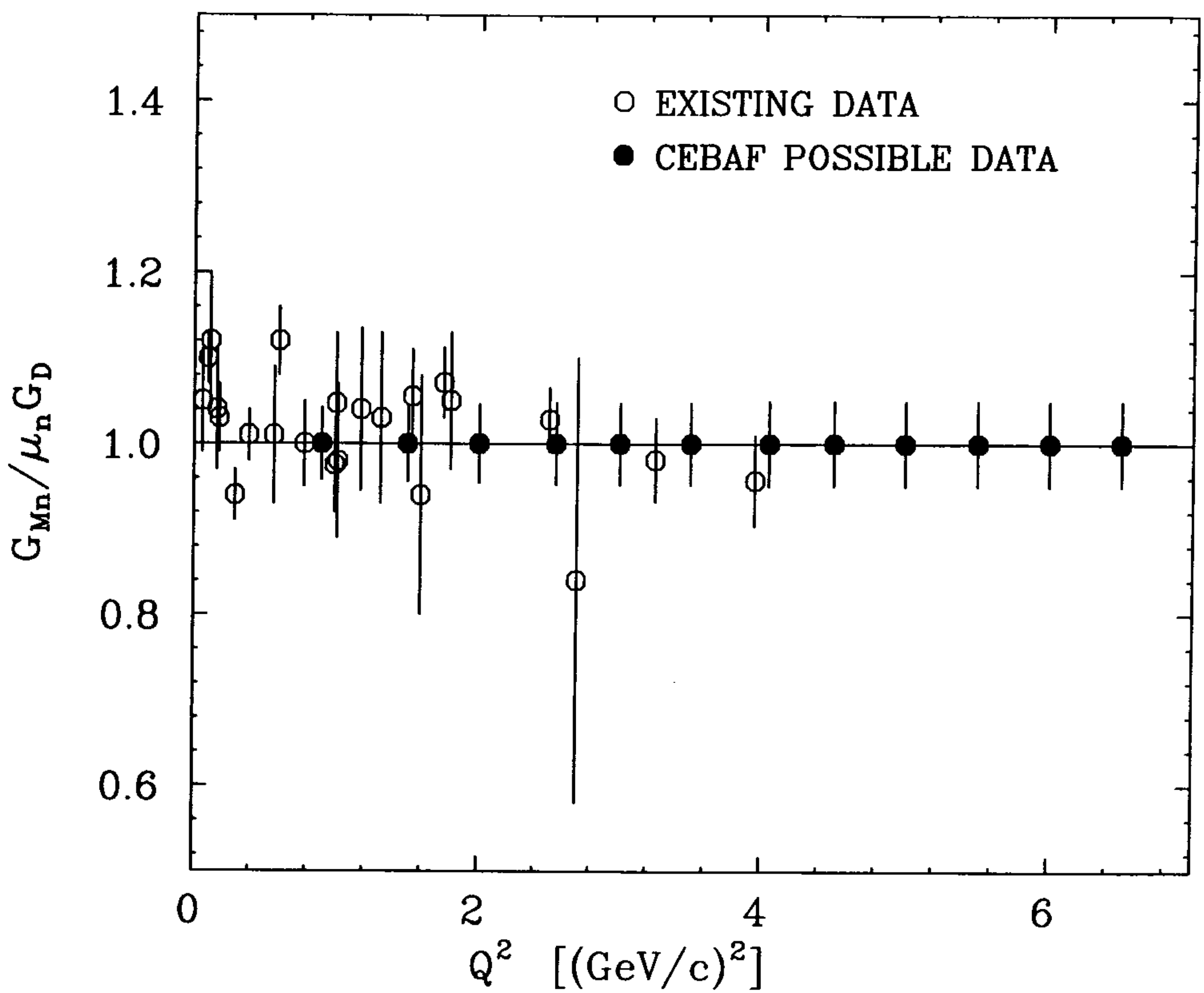

EXISTING DATA
CEBAF POSSIBLE DATA
1.4
1.2
1.0
0.8
0.6
$G_{Mn}/\mu_n G_D$
0
2
4
6
Q^2 [(GeV/c)^2]

Figure 6